Partial Inverse Compensation Techniques for Linear Control Design in Magnetostrictive Transducers

James Nealis[1] and Ralph C. Smith[2]

Center for Research in Scientific Computation, North Carolina State Univ., Raleigh, NC 27695

Abstract

This paper focuses on the development of partial inverse compensation techniques for linear control design in systems employing magnetostrictive transducers operating in nonlinear and hysteretic regimes. At low drive levels, linear models can be used to characterize strains and forces generated by magnetostrictive transducers with reasonable accuracy. However, at the moderate to high drive levels where transducer performance is optimal, inherent constitutive nonlinearities and hysteresis must be accommodated to achieve the accuracy and speed requirements for high performance applications. Appropriate nonlinear and hysteretic modeling techniques are reviewed and an inverse compensator based on the nonlinear kernel of the model is developed. The performance of the technique is illustrated through numerical examples.

Keywords: Inverse compensator, nonlinear and hysteretic regimes, magnetostrictives

1. Introduction

Magnetostrictive transducers have been increasingly employed in certain industrial and automotive processes due to the magnitude of forces and strains which can be generated through currents applied to a surrounding solenoid. To achieve bidirectional forces and strains, the actuator inputs are typically biased through either an applied DC current to the solenoid or by way of a permanent magnet surrounding the solenoid. Even in this biased state, however, the transducers exhibit hysteresis and constitutive nonlinearities which must be accommodated in both models and control designs to achieve the speed and accuracy specifications for high performance applications.

A variety of modeling approaches have been employed to quantify magnetostrictive transducer dynamics including Preisach models [1, 3, 10, 12, 13] and quasi-macroscopic models based on domain wall properties of the constituent materials [4, 5, 6, 7, 21]. A property of both approaches is the fact that associated inverse models can be constructed to build full inverse compensators for linear control design. However, the nature of the full inverse models differs substantially for the two approaches. Due to the algebraic nature of Preisach models, algebraic inverse models can be constructed for arbitrary initial conditions. The models based on domain wall dynamics have the form of differential equations which evolve as a function of the input field or time. This yields inverse models posed in terms of a complementary differential equation. There exist advantages and disadvantages to both approaches for constructing models and inverse compensators; however, in both cases the complexity in constructing a full inverse provides a significant technological challenge when experimentally implementing the compensator. Furthermore, this complexity

---

[1]Email: jmnealis@unity.ncsu.edu, Telephone: (919) 515-7234
[2]Email: rsmith@eos.ncsu.edu; Telephone: (919) 515-7552

1. REPORT DATE **2001**	2. REPORT TYPE	3. DATES COVERED **00-00-2001 to 00-00-2001**

4. TITLE AND SUBTITLE **Partial Inverse Compensation techniques for Linear Control Design in Magnetostrictive Transducers**	5a. CONTRACT NUMBER
	5b. GRANT NUMBER
	5c. PROGRAM ELEMENT NUMBER
6. AUTHOR(S)	5d. PROJECT NUMBER
	5e. TASK NUMBER
	5f. WORK UNIT NUMBER

7. PERFORMING ORGANIZATION NAME(S) AND ADDRESS(ES) **North Carolina State University,Center for Research in Scientific Computation,Raleigh,NC,27695-8205**	8. PERFORMING ORGANIZATION REPORT NUMBER
9. SPONSORING/MONITORING AGENCY NAME(S) AND ADDRESS(ES)	10. SPONSOR/MONITOR'S ACRONYM(S)
	11. SPONSOR/MONITOR'S REPORT NUMBER(S)

12. DISTRIBUTION/AVAILABILITY STATEMENT **Approved for public release; distribution unlimited**

13. SUPPLEMENTARY NOTES

14. ABSTRACT **see report**

15. SUBJECT TERMS

16. SECURITY CLASSIFICATION OF:			17. LIMITATION OF ABSTRACT	18. NUMBER OF PAGES **12**	19a. NAME OF RESPONSIBLE PERSON
a. REPORT **unclassified**	b. ABSTRACT **unclassified**	c. THIS PAGE **unclassified**			

leads to significant robustness issues when designing compensators which must perform under a variety of operating conditions.

An alternative approach is to employ partial compensators which incorporate the primary nonlinear mechanisms but are sufficiently efficient and robust to permit real-time implementation in physical systems. In this paper we consider a partial inverse compensator based on the anhysteretic (hysteresis-free) component of recently developed domain wall models for magnetostrictive transducers. This incorporates the nonlinear behavior of the transducer, including saturation nonlinearities, but neglects the hysteresis inherent to the system. It is illustrated through numerical examples that the unincorporated hysteresis, which introduces phase delays into the transducer dynamics, can be successfully attenuated through feedback mechanisms when employed in combination with the partial inverse compensator. This yields a control design which is sufficiently efficient and robust to experimentally implement, as illustrated in [14] where an analogous design was employed.

The nonlinear anhysteretic model, fully coupled hysteresis model, inverse compensators, and commensurate numerical techniques are summarized in Section 2 for a prototypical magnetostrictive transducer design. In modeling the transducer, care is taken to couple the nonlinear magnetomechanical effects with the elastic properties of the transducer. A proportional-integral-derivative (PID) control design which incorporates the partial compensator is discussed in Section 3 and illustrated through numerical examples in Section 4. Specifically, it is illustrated that through linear control design in combination with the partial compensator, highly accurate displacements are achieved even while operating the transducer in highly nonlinear and hysteretic regimes.

2. Transducer Model and Inverse Compensators

We consider here the development of a model and inverse compensator for the prototypical magnetostrictive transducer depicted in Figure 1. This design is representative of transducers commonly employed in both academic and industrial applications. Input fields are provided by the application of a current to the solenoid surrounding a Terfenol-D rod. Prestress mechanisms are employed to further align domains perpendicular to the longitudinal rod axis and to maintain the rod in compression. The mass at the end of the rod provides a lumped model of structural components driven by the actuator. The permanent magnet surrounding the solenoid provides a bias field to achieve bidirectional strains and forces and can also be employed for flux shaping to minimize end effects in the rod.

The model will be developed in four steps; (i) quantification of the anhysteretic magnetization M_{an}, (ii) quantification of the total magnetization M, (iii) characterization of the free strains, or magnetostriction λ, and (iv) characterization of the full strains e and displacements at the rod tip. All components of the
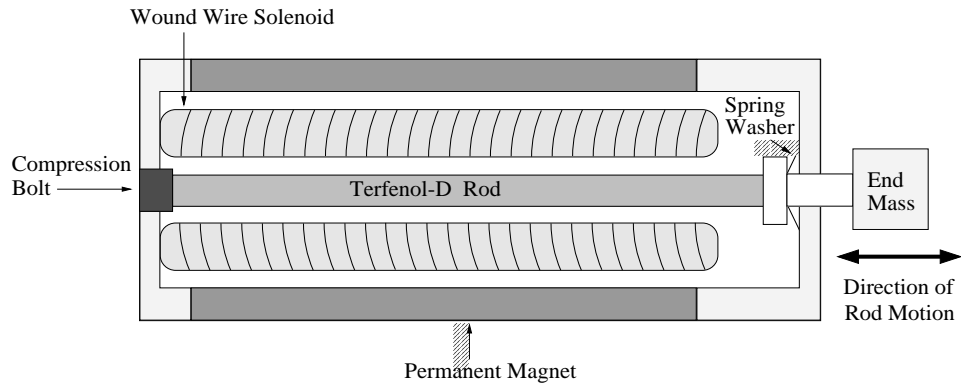
Figure 1. Cross section of a prototypical Terfenol-D magnetostrictive transducer.

model have been developed in previous investigations and only those details pertinent to the development and testing of the inverse compensator will be included.

The anhysteretic magnetization M_{an} can be interpreted as the locus of values obtained if a decaying AC field (or stress) superimposed on a DC field (or stress) is employed to obtain minimum magnetization or energy states. Physically, the anhysteretic magnetization can be interpreted as the magnetization obtained when domain walls are translated across pinning sites to obtain a minimum energy state [8].

For the model described here, Boltzmann statistics are used to balance the thermal and magnetostatic energies in order to quantify the anhysteretic magnetization. Under the assumption of uniform dipole orientation, this yields the Langevin model

$$M_{an} = M_s \left[\coth(H_e/a) - (a/H_e) \right], \tag{1}$$

whereas the Ising model

$$M_{an} = M_s \tanh(H_e/a) \tag{2}$$

results from the assumption that dipoles can align only in the direction of the applied field or opposite to it. Here M_s denotes the saturation magnetization, a is temperature-dependent coefficient, and

$$H_e = H + \alpha M + H_\sigma \tag{3}$$

is the effective field observed in domains. In the latter expression, H is the field generated by the solenoid, α is a coupling coefficient which quantifies field effects due to neighboring dipoles, and H_σ is the field generated by stresses in the material. We note that while the expressions (1) and (2) are equivalent through third-order terms, the Ising relation (2) is advantageous for inverse compensator design since it can be inverted to yield

$$H = a \cdot \operatorname{arctanh}(M_{an}/M_s) - \alpha M_{an} - H_\sigma . \tag{4}$$

Expression (4) provides the basis for constructing a partial inverse compensator for linear control design.

To quantify the total magnetization M generated in the Terfenol-D rod, it is necessary to also incorporate the reversible and irreversible magnetization M_{rev} and M_{irr} respectively due to domain wall bending and translation across pinning sites. As detailed in [8, 9] for general magnetic materials and [4, 5, 6, 7] for magnetostrictive transducers, the use of magnetostatic principles to compute the energy required to reorient dipoles in order to model domain wall motion yields the differential equation

$$\frac{dM_{irr}}{dH} = \widehat{\delta} \frac{M_{an} - M_{irr}}{k\delta - \alpha(M_{an} - M_{irr})} . \tag{5}$$

The constant k quantifies irreversible effects, $\delta = \operatorname{sign}(H)$ guarantees that the energy required to break pinning sites always opposes the field, and

$$\widehat{\delta} = \begin{cases} 1 & , \quad (dH > 0 \text{ and } M \leq M_{an}) \text{ or } (dH < 0 \text{ and } M \geq M_{an}) \\ 0 & , \quad \text{otherwise} \end{cases}$$

enforces reversible domain wall motion during initial field reversal. When combined with the algebraic relation

$$M_{rev} = c(M_{an} - M_{irr}), \tag{6}$$

where c is a reversibility coefficient, this yields the expression

$$M = (1 - c)M_{irr} + cM_{an} \tag{7}$$

for the total magnetization. The relation (7) is typically employed for material characterization.

For compensator design, it is advantageous to reformulate (7) as

$$\frac{\partial M}{\partial H} = F(H, M)$$

$$M(H_0) = M_0$$

(8)

where

$$F(H, M) = \frac{1}{1 + c\alpha \frac{\partial M_{an}}{\partial H}} \left[\hat{\delta} \frac{M_{an} - M}{k\delta - \hat{\alpha}(M_{an} - M)} + c\frac{\partial M_{an}}{\partial H} \right]$$

(9)

where $\hat{\alpha} = \frac{\alpha}{1-c}$ and M_{an} is specified by either (1) or (2). A model inverse is then specified by the complementary differential equation

$$\frac{\partial M^{-1}}{\partial H} = \frac{1}{F(M^{-1}, H)}$$

$$M^{-1}(H_0) = M_1 \,.$$

(10)

This provides an exact inverse if the parameters M_s, α, a, c and k are known exactly or an approximate inverse if the parameters are unknown or slowly varying due to operating conditions. We note that while the inverse (10) has been experimentally implemented [19], highly accurate initial conditions for (10) must be obtained in order to achieve accurate compensation for the hysteresis and constitutive nonlinearities. This promotes the use of partial compensators based on (4).

The expressions (7) or (8) quantify the relation between the field generated in the Terfenol-D rod and the resulting magnetization. It is next necessary to quantify the strains, forces, and displacements generated by the change in magnetization. This is considered in two steps: (i) quantify the free strains in the material and (ii) quantify the total strains which also include elastic effects.

For an unbiased actuator, the free strains, or magnetostriction, can be characterized by the quadratic relation

$$\lambda(t) = \frac{3\lambda_s}{2M_s^2} M^2$$

(11)

where λ_s denotes the saturation magnetostriction. To achieve bidirectional strains or forces, the transducer is biased by the surrounding magnet or the application of a DC field to the solenoid. For a bias of $M_s/2$, the free strains are modeled by

$$\lambda(t) = \frac{3\lambda_2}{2M_s^2} \left[M^2(t) + 2M_s M(t) \right]$$

(12)

with similar relations resulting from more general bias levels.

The relation (12) quantifies the free strains due to the rotation of dipoles and hence changes in magnetization but it does not incorporate elastic properties of the Terfenol-D rod and prestress springs nor does it incorporate the inertial effects due to the lumped masses at the end of the rod. The incorporation of these effects requires the generalization of the linear relation

$$\varepsilon = s^H \sigma + d_{33} H$$

where ε and σ respectively denote the strain and stress, s^H is the compliance at constant field, and d_{33} is a linear coupling coefficient, to accommodate the previously modeled constitutive nonlinearities and hysteresis. This is accomplished by replacing $d_{33}H$ by λ specified in (12) and considering the dynamic equations for the rod. The development of this component of the model is detailed in [5, 7].

For the quantification of total strains and resulting displacements, we consider the rod to be fixed at the left end $(x = 0)$ while the right end $(x = L)$ is constrained by a damped oscillator and has an attached point mass M_L as depicted in Figure 2. The density, Young's modulus and internal damping coefficients
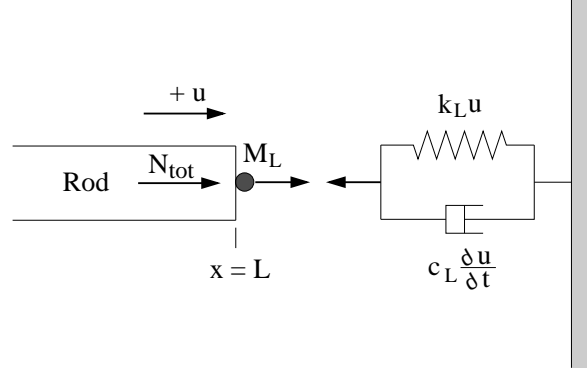
Figure 2. Orientation of spring forces, edge reactions and resultants for the Terfenol rod.

for the rod are respectively denoted by ρ, E and c_D. The prestress spring is assumed to have stiffness k_ℓ and Kelvin-Voigt damping coefficient c_L.

Under the assumption of linear elasticity, Kelvin-Voigt damping, and small displacements, the stress at any point $x, 0 \leq x \leq L$, is given by

$$\sigma(t, x) = E\frac{\partial u}{\partial x}(t, x) + c_D\frac{\partial^2 u}{\partial x \partial t}(t, x) - E\lambda(t, x) \tag{13}$$

where $u(t, x)$ denotes the longitudinal displacement and $\lambda(t, x) = \lambda(t)$ is given by (12). We assume that the magnetostriction is uniform along the length of the rod. This assumption is reasonable in present actuator designs since flux shaping via the surrounding magnet can be used to minimize end effects in the rod.

Force balancing then yields

$$\rho A\frac{\partial^2 u}{\partial t^2} = \frac{\partial N_{tot}}{\partial x} \tag{14}$$

where the resultant is specified by

$$N_{tot} = EA\frac{\partial u}{\partial x} + c_D A\frac{\partial^2 u}{\partial x \partial t} - EA\lambda\,.$$

To obtain appropriate boundary conditions, we first note that $u(t, 0) = 0$. Force balancing at $x = L$ yields

$$N_{tot}(L, t) = -k_L u(t, L) - c_L\frac{\partial u}{\partial t}(t, L) - M_L\frac{\partial^2 u}{\partial t^2}(t, L)\,.$$

The initial conditions are taken to be $u(0, x) = \frac{\partial u}{\partial x}(0, x) = 0$.

To pose the PDE (14) in a form which facilitates approximation, we consider a weak form of the model with state space $X = L^2(0, L)$ and the space of test functions is taken to be $V = H_L^1(0, L) \equiv \{\phi \in H^1(0, L) \,|\, \phi(0) = 0\}$. Multiplication by test functions followed by integration then yields the weak form

$$\int_0^L \rho A\frac{\partial^2 u}{\partial t^2}\phi\,dx = -\int_0^L EA\frac{\partial u}{\partial x}\frac{\partial \phi}{\partial x}\,dx - \int_0^L c_D A\frac{\partial^2 u}{\partial x \partial t}\frac{\partial \phi}{\partial x}\,dx + \int_0^L EA\lambda\frac{\partial \phi}{\partial x}\,dx$$
$$- \left[k_L u(t, L) + c_L\frac{\partial u}{\partial t}(t, L) + M_L\frac{\partial^2 u}{\partial t^2}(t, L)\right]\phi(L) \tag{15}$$

which must be satisfied for all $\phi \in V$.

For either simulation purposes or control implementation, it is necessary to discretize the infinite dimensional model (15). This is accomplished by employing a Galerkin discretization in space and a finite difference approximation in time. To define a finite element discretization in space, we consider a uniform partition of the interval $[0, L]$ and consider a basis $\{\phi_i\}_{i=1}^N$ comprised of of linear splines

$$\phi_i(x) = \frac{1}{h} \begin{cases} (x - x_{i-1}) \ , \ x_{i-1} \leq x < x_i \\ (x_{i+1} - x) \ , \ x_i \leq x \leq x_{i+1} \\ 0 \ , \ \text{otherwise} \end{cases} \ , \quad i = 1, \cdots, N-1$$

$$\phi_N(x) = \frac{1}{h} \begin{cases} (x - x_{N-1}) \ , \ x_{N-1} \leq x \leq x_N \\ 0 \ , \ \text{otherwise} \end{cases}$$

(see [11] for details).

The solution $u(t, x)$ to (15) is then approximated by the expansion

$$u^N(t, x) = \sum_{j=1}^N u_j(t) \phi_j(x) \,.$$

Because $H^N = \text{span}\{\phi_i\}_{i=1}^N \subset H_L^1(0, L)$, the approximate solution satisfies the essential boundary condition $u^N(t, 0) = 0$ and can attain arbitrary displacements at $x = L$.

The projection of the problem (15) onto the finite dimensional subspace H^N yields the second-order semidiscrete system

$$Q\ddot{\vec{u}}(t) + C\dot{\vec{u}}(t) + K\vec{u}(t) = \vec{f}(t) \tag{16}$$

where $\vec{u}(t) = [u_1(t), \cdots, u_N(t)]$. The mass, stiffness and damping matrices have the components

$$[Q]_{ij} = \begin{cases} \int_0^L \rho A \phi_i \phi_j \, dx \ , \quad i \neq n \text{ or } j \neq n \\ \int_0^L \rho A \phi_i \phi_j \, dx + M_L \ , \quad i = n \text{ and } j = n \end{cases}$$

$$[K]_{ij} = \begin{cases} \int_0^L EA \phi_i' \phi_j' \, dx \ , \quad i \neq n \text{ or } j \neq n \\ \int_0^L EA \phi_i' \phi_j' \, dx + k_L \ , \quad i = n \text{ and } j = n \end{cases}$$

$$[C]_{ij} = \begin{cases} \int_0^L c_D A \phi_i' \phi_j' \, dx \ , \quad i \neq n \text{ or } j \neq n \\ \int_0^L c_D A \phi_i' \phi_j' \, dx + c_L \ , \quad i = n \text{ and } j = n \end{cases}$$

while the force vector is defined by

$$[\vec{f}(t)]_i = \int_0^L EA\lambda(t, x) \phi_i'(x) \, dx \,.$$

Letting $\vec{y}(t) = [\vec{u}(t), \dot{\vec{u}}(t)]^T$ and

$$A = \begin{bmatrix} 0 & I \\ -M^{-1}K & -M^{-1}C \end{bmatrix} \ , \quad \vec{F}(t) = \begin{bmatrix} 0 \\ M^{-1}\vec{f}(t) \end{bmatrix} \,,$$

the second-order system (16) can be posed as the first-order system

$$\dot{\vec{y}}(t) = A\vec{y}(t) + \vec{F}(t)$$
$$\vec{y}(0) = \vec{y}_0 \,,$$

(17)

where the $2N \times 1$ vector $\vec{y}_0$ denotes the projection of the initial conditions into the approximation space.

The system (17) can be employed for finite-dimensional control design. For subsequent implementation, we consider a temporal discretization of (17) using a modified trapezoid rule. For temporal stepsizes Δt, this yields the difference equations

$$\vec{y}_{j+1} = \mathcal{A}\vec{y}_j + \mathcal{F}\vec{F}(t_j)$$
$$\vec{y}_0 = \vec{y}(0) \,,$$

(18)

where $t_j = j\Delta t$, $\vec{y}_j$ appoximates $\vec{y}(t_j)$ and

$$\mathcal{A} = \left[I - \frac{\Delta t}{2}A\right]^{-1} \left[I + \frac{\Delta t}{2}A\right] \quad , \quad \mathcal{F} = \Delta t \left[I - \frac{\Delta t}{2}A\right]^{-1} .$$

This yields an A-stable, single step method requiring moderate storage and providing moderate accuracy.

3. Control Design

We summarize here the design of control laws which utilize the partial inverse compensator. The emphasis is to illustrate the flexibility of the compensator for general purpose control methods rather than optimal control design; hence we consider a proportional-integral-derivative (PID) controller which utilizes the partial inverse compensator. The performance of the partial compensator when incorporated in more sophisticated control laws will be reported in future works.

The general form of the PID controller employed here is

$$u(t) = k \left[e(t) + \frac{1}{T_i} \int_0^t e(s)ds + T_d\frac{de}{dt}(t)\right]$$

(19)

where k, T_i and T_d are gains and $e(t)$ is the error between the desired signal and the system output. For the application described in the next section, the error is defined to be the difference between the desired and measured positions of a cutting head fastened to the end of the Terfenol-D rod in the transducer depicted in Figure 1. Hence the errors are given by

$$e(t) = u_d(t) - u(t, L)$$

where u_d is the desired position of the rod tip and $u(t, L)$ denotes the solution to the modeling differential equation (15). The latter incorporates the constitutive nonlinearities and hysteresis inherent to the transducer through the input term $\lambda(t)$ defined in (12).

As illustrated in Figure 3, the partial compensator

$$M^{-1} = a \cdot \text{arctanh}(H/M_s) - \alpha H - H_\sigma \,,$$

which is derived from (4), is employed as a filter before the nonlinear and hysteretic transducer model (or physical actuator). This filter accommodates the constitutive nonlinearities, including saturation effects, but does not compensate for hysteresis.

The standard method for determining the gains k, T_i and T_d, as described in [2], is to introduce a step input to the system and find the point of maximal slope for the system response. The intercepts of the tangent line at this point with the coordinate axes provide the parameters used to determine gains.
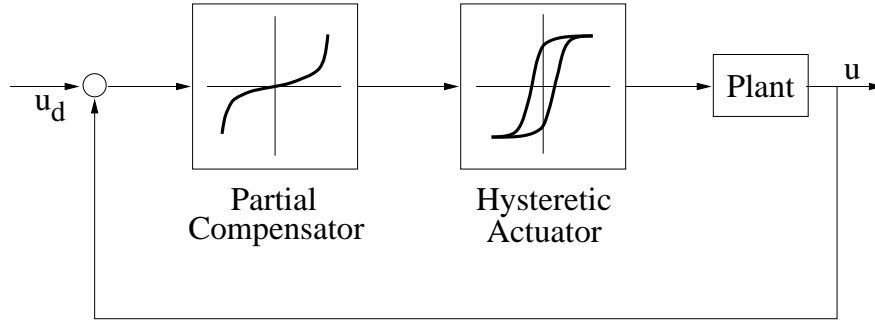
Figure 3. Control design utilizing a partial inverse compensator in a system with nonlinear and hysteretic actuators.

Numerical examples have illustrated, however, that further tuning of parameters from the initially prescribed values will significantly improve the performance of the method. This is partially due to the phase delays associated with uncompensated hysteresis and the large difference in magnitude between the output and input signals. The errors due to phase delays affect the integral component of the control in a manner similar to that described in [2].

4. Numerical Examples

To illustrate the control methodology, we consider a prototypical application similar to that developed at Etrema Products [3]. As depicted in Figure 4, a magnetostrictive transducer is employed to mill out-of-round objects. To attain production specifications, milling is performed at a rate of 3000 rpm with cutting tolerances of ± 1 micron. Details regarding the experimental implementation of a control law employing an analogous compensator can be found in [14].

For the numerical simulations reported here, periodic signals modeling potential cutting trajectories were specified for $u_d(t)$. The parameter values $\rho = 9250$ kg/m^2, $E = 3 \times 10^{10}$ N/m^2, $c_D = 3 \times 10^6$ Ns/m^2, $M_L = 0.5$ kg, $k_L = 2 \times 10^6$ N/m and $c_L = 1 \times 10^3$ Ns/m were employed in the model (15) quantifying the displacements generated by the transducer. These values were obtained when characterizing the transducer reported in [7] and hence are typical for transducers of the type employed in milling applications. The parameters in the hysteresis model were taken to be $M_s = 7.65 \times 10^5$ A/m, $\alpha = -.01$, $c = 0.18$, $k = 4000$ A/m and $a = 7012$ A/m. As noted in [5, 7], these choices are also commensurate with values obtained when characterizing physical transducers.
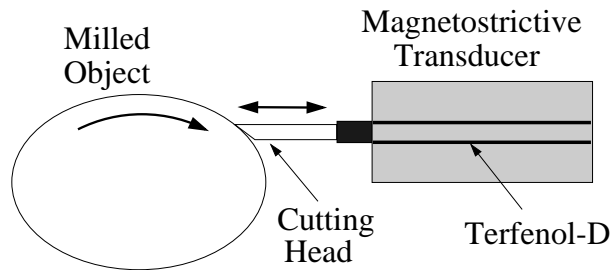
Figure 4. High speed milling application.

$x\,10^4$ (top left) ... $x\,10^{-5}$ (top right)

(a)   (b)
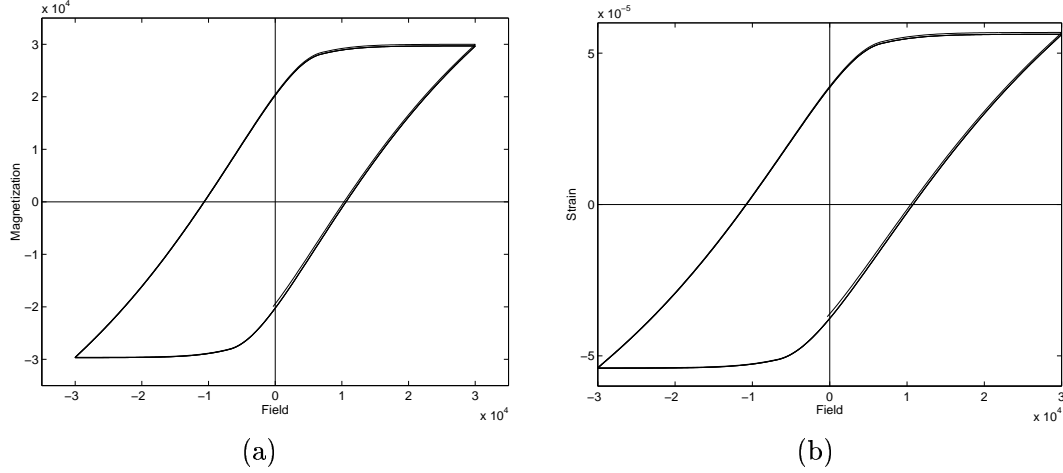
Figure 5. (a) Hysteretic relationship between the input field H and magnetization M modeled by (7); (b) Relationship between H and the strain $\varepsilon = u(t, L)/L$ given by (15).

We consider first the tracking of a single frequency, sinusoidal trajectory $u_d(t)$. The modeled magnetization and strain resulting respectively from (7) and (15) are plotted in Figure 5. Both relations illustrate the significant hysteresis and constitutive nonlinearities inherent to the system. The commanded position $u_d(t)$ and measured position $u(t, L)$, in the absence of feedback control or inverse compensation, are plotted versus each other in Figure 6a and as a function of time in Figure 6b. The first plot illustrates the hysteretic relationship between the two trajectories while the second plot illustrates the resulting phase delays and nonlinear saturation effects. The accuracy in this case is significantly worse than that specified for the product.

The analogous trajectories obtained with the PID control law (19) employing the partial compensator depicted in Figure 3 are plotted in Figure 7. In this case, a nearly linear relation is maintained between the commanded and measured trajectories, and the maximum absolute error over the time interval $[0, 25]$ is 3.37×10^{-8}.

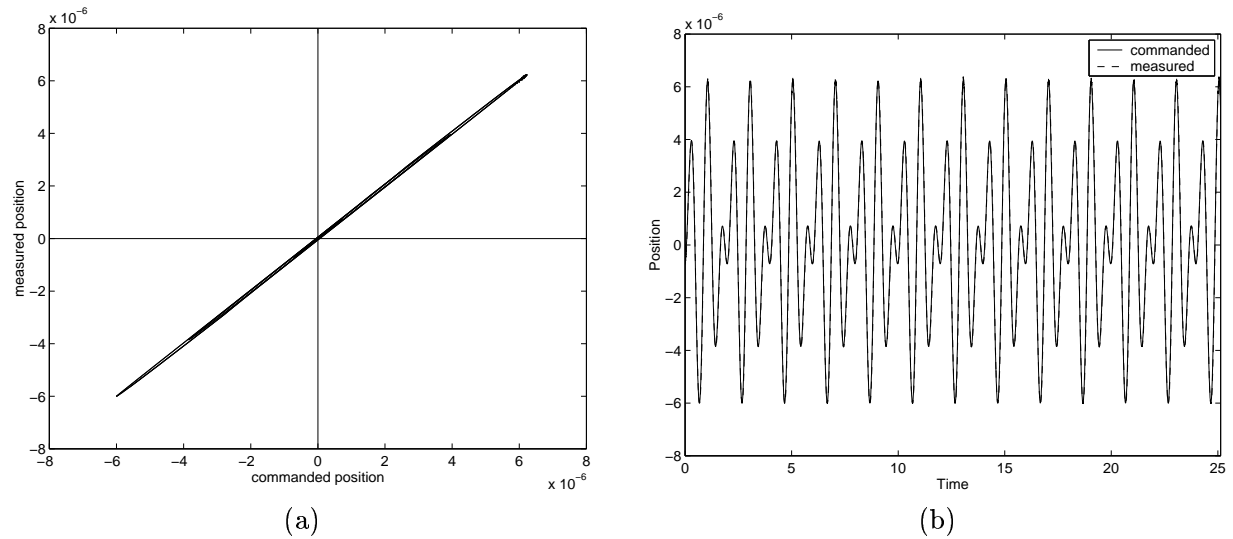(a)   (b)
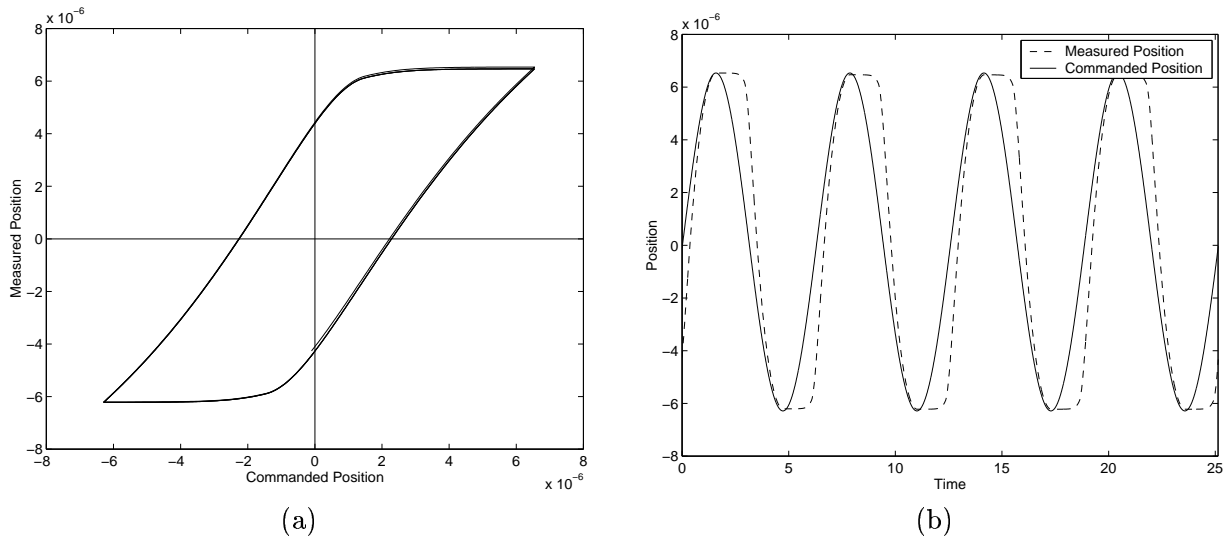
Figure 6. (a) Relationship between the measured and commanded positions in the absence of partial compensation or feedback; (b) Measured and commanded positions as a function of time.

(a)

(b)
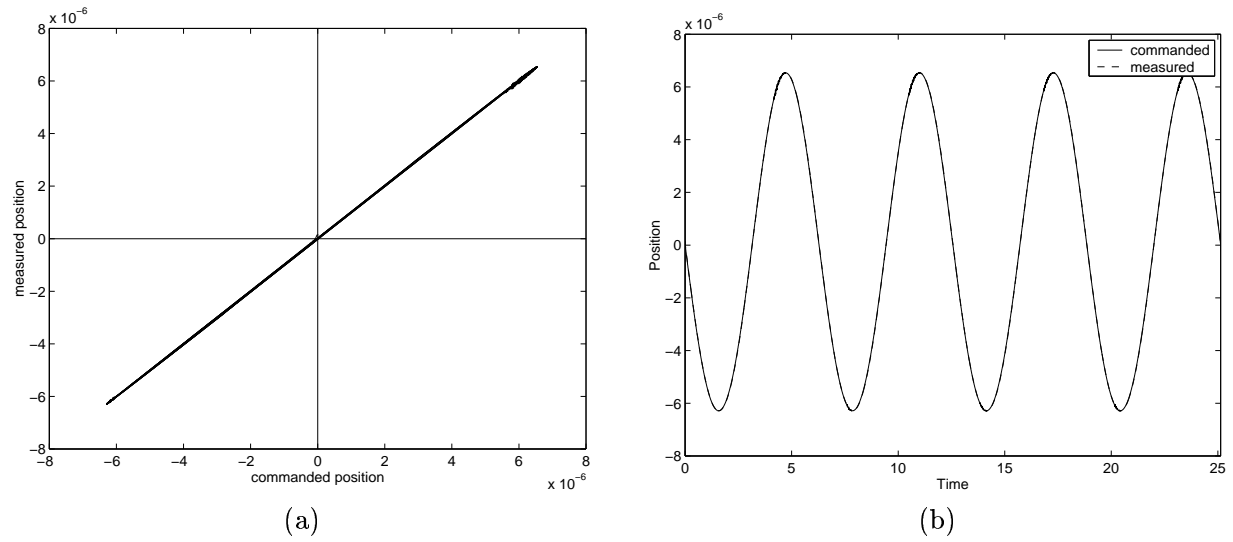
Figure 7. (a) Relationship between the measured and commanded positions with partial compensation and feedback; (b) Measured and commanded positions as a function of time.

The performance of the control design for tracking trajectories comprised of multiple frequencies is illustrated in Figure 8. Figure 8a illustrates that a nearly linear relation between the commanded and measured positions is again maintained in spite of the hysteresis and constitutive nonlinearities inherent to the actuator and incorporated in the actuator model. The maximum absolute error between the trajectories plotted in Figure 8b is 1.04×10^{-7} for this simulation. In both cases, the PID controller employing the partial compensator is effectively attenuating the constitutive nonlinearities and hysteresis associated with the transducer.

(a)

(b)

Figure 8. (a) Relationship between the measured and commanded positions with partial compensation and feedback for two frequencies; (b) Measured and commanded positions as a function of time.

5. Concluding Remarks

This paper illustrates the construction of a partial inverse compensator for linear control design in systems utilizing magnetostrictive transducers operating in nonlinear and hysteretic regimes. This compensator is based on the anhysteretic magnetization which provides the nucleus for a variety of hysteresis models based on domain wall properties of the constituent materials. Hence the partial compensator arises naturally as one component of the model employed for full material characterization. While less accurate than full inverse compensators based on complete hysteresis models, the simplicity of the partial compensator facilitates experimental implementation and promotes robustness.

The performance of the partial compensator when employed in concert with a PID control law was illustrated through numerical simulation to be highly accurate for the considered examples. Similar results have been obtained experimentally with an analogous construction for a partial inverse [14]. In combination, these results attest to the capabilities of the method for linear control design in high performance systems utilizing magnetostrictive actuators operating in nonlinear and hysteretic regimes.

Finally, analogous models have been developed for ferroelectric devices including piezoceramics [17, 18] and relaxor ferroelectric materials [15, 16], and analogous control methodologies for these materials are currently being developed.

Acknowledgements

References

[1] A. Adly, I. Mayergoyz and A. Bergqvist, "Preisach modeling of magnetostrictive hysteresis," *J. Appl. Phys.*, 69(8), pp. 5777-5779, 1991.

[2] K.J. Astrom and T. Hagglund, "Automatic Tuning of PID controllers," Instrument Society of America, Raleigh, NC, 1988.

[3] V. Basso and G. Bertotti, "Hysteresis models for the description of domain wall motion," *IEEE Trans. Magn.*, 32(5) pp. 4210-4213, 1996.

[4] F.T. Calkins, R.C. Smith and A.B. Flatau. "An energy-based hysteresis model for magnetostrictive transducers," *IEEE Transactions on Magnetics.* 36(2), pp. 429-439, 2000.

[5] M.J. Dapino, R.C. Smith, L.E. Faidley and A.B. Flatau, "A coupled structural-magnetic strain and stress model for magnetostrictive transducers," *Journal of Intelligent Material Systems and Structures*, 11(2), 2000, pp. 134-152.

[6] M.J. Dapino, R.C. Smith and A.B. Flatau. "An active and structural strain model for magnetostrictive transducers." Proceedings of the SPIE, Smart Structures and Integrated Systems, San Diego, CA, 1998, Vol. 3329, pp. 198-209.

[7] M.J. Dapino, R.C. Smith and A.B. Flatau. "A structural-magnetic strain model for magnetostrictive transducers," *IEEE Transactions on Magnetics*, 36(3), pp. 545-556, 2000.

[8] D.C. Jiles. *Introduction to Magnetism and Magnetic Materials.* Chapman and Hall, New York, 1991.

[9] D.C. Jiles and D.L. Atherton, "Theory of ferromagnetic hysteresis," *Journal of Magnetism and Magnetic Materials*, 61, pp. 48-60, 1986.

[10] D.A. Philips, L.R. Dupré and J.A. Melkebeek, "Comparison of Jiles and Preisach hysteresis models in magnetodynamics," *IEEE Trans. Magn.*, 31(6), pp. 3551-3553, 1995.

[11] P.M. Prenter, *Splines and Variational Methods*, Wiley, New York, 1975.

[12] J.B. Restorff, H.T. Savage, A.E. Clark and M. Wun-Fogle. "Preisach modeling of hysteresis in Terfenol-D," *Journal of Applied Physics*, 67(9), pp. 5016-5018, 1996.

[13] R.C. Smith, "Hysteresis modeling in magnetostrictive materials via Preisach operators." *Journal of Mathematical Systems, Estimation and Control*, 8(2), summary pp. 249-252, 1998.

[14] R.C. Smith, C. Bouton and R. Zrostlik, "Partial and full inverse compensation for hysteresis in smart material systems," Proceedings of the 2000 American Control Conference.

[15] R.C. Smith and C.L. Hom, "Domain wall theory for ferroelectric hysteresis," *Journal of Intelligent Material Systems and Structures*, 10(3), 1999, pp. 195-213.

[16] R.C. Smith and C.L. Hom, "A temperature-dependent hysteresis model for relaxor rerroelectrics," Proceedings of the SPIE, Smart Structures and Materials 2000, Newport Beach, CA, Volume 3992, pp. 267-278, 2000.

[17] R.C. Smith and Z. Ounaies, "A domain wall model for hysteresis in piezoelectric materials," *Journal of Intelligent Material Systems and Structures*, 11(1), 2000, pp. 62-79.

[18] R.C. Smith, Z. Ounaies and R. Wieman, "A model for rate-dependent hysteresis in piezoceramic materials operating at low frequencies," Proceedings of the SPIE, Smart Structures and Materials 2000, Newport Beach, CA, Volume 3992, pp. 128-136, 2000.

[19] R.C. Smith and R. Zrostlik, "Inverse compensation for ferromagnetic hysteresis," CRSC Technical Report CRSC-TR99-28; Proc. 38th IEEE Conf. Dec. and Control, Phoenix, AZ, 1999.

[20] G. Tao and P.V. Kokotovic, *Adaptive Control of Systems with Actuator and Sensor Nonlinearities*, John Wiley and Sons, New York, 1996.

[21] R. Venkataraman and P. Krishnaprasad, "A model for a thin magnetostrictive actuator," in *Proceedings of the Conference on Information Sciences and Systems*, 1998.